II－3

# Shoreline Changes around the Mu-River Mouth

Zhaowu MENG, Satoshi TOHMA, Hideo KONDO
Muroran Institute of Technology
Hiroshi HASEGAWA
Hokkaido Developing Consultant Company

**Abstract** Changes of shoreline around the Mu-River mouth from Feb. to Aug. 1996 are reproduced by one-line model. In one-line model regular and irregular wave deformation computing are carried out before searching breaking points. As a result, except for extremely unusual wave conditions, the utility of one-line model is verified on the shoreline changes around the Mu-River mouth.

## 1. Introduction

The Mu-River mouth is located in the South Hokkaido, and faced to the Pacific Ocean. The peak discharge happened on Aug. 10, 1992, it reached 2,971m³/s; and the minimum one is only 1.31m³/s, occurred on Aug. 18, 1982. On an average its discharge is 36.5m³/s. It transports sand to the sea in traction state 500m³/year, and 800,000m³/year in suspension.[1-2)]

Shoreline around the river mouth has being eroded since 1967. The predominant direction of littoral drift is westward, that is from the left hand side to the right hand side of the river mouth. 1978, however, is the year that speed on recession of two sides of the river mouth changed. Before 1978, recession speed on the right hand side was about 13m/year, and one on the left hand side was 4m/year. Whereas, since 1978 to 1985, recession speed on the right hand side became about 27m/year, and one on the left hand side became 4m/year around. Very fast erosion on the left hand side was resulted in by construction of the Shiomi Fishery Port. As this port interrupted the natural balance of littoral drift around the river mouth: While on an average wave-energy conditions are still the same every year. Thus, sand is stopped and deposited on the east of the port, but unchanged average wave-forces transport sand on the left hand side of the river mouth to the right hand side, and further westward. Since 1985, shoreline erosion has been reinstated as during the period from 1967 to 1978.

Although mechanism on sand transportation is hard to understand, many propositions have been well made to quantify relation between shoreline changes and wave conditions.[3-6)] CERC's formulae is the best one to be applied in many coastal areas in the world. Kosasa and Bramton improved it based on changes of wave heights at breaking points, Kraus successfully confirmed its applicability at Oarai Beach, Japan.[5)] In order to understand mechanism of the variation of shoreline better, the above researches are applied in one-line model with regular and irregular wave deformation model to reproduce changes of shoreline around the Mu-River mouth from Feb. to Aug. 1996.

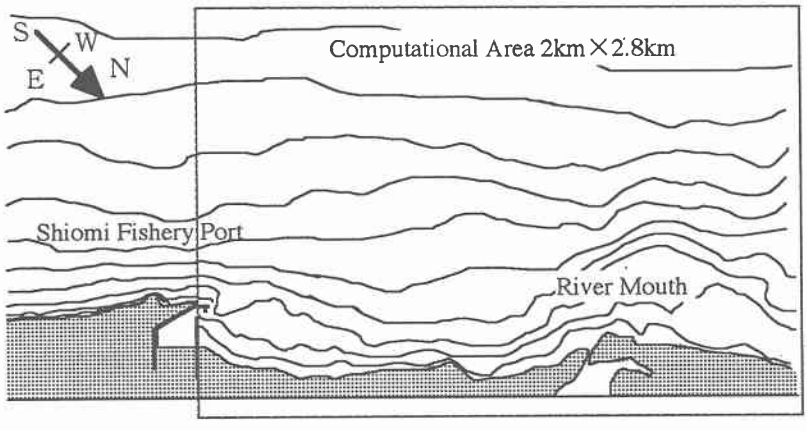


**Fig. 1 Bathymetry around the Mu-River Mouth(Feb. 1996)**

鵡川河口周辺の汀線変化
孟昭武、藤間聡、近藤俶郎、長谷川裕史

## 2. Wave characteristics

It is important to study dangerous waves induced by such as typhoons or tsunamis when making shore erosion countermeasures. It is essential, however, to consider representative waves that make long-term variation of shore morphology.

No field data on waves around the Mu-River mouth have been observed. In this research, significant waves around the East Tomakomai Harbor that 25km west to, and the Tomihama Harbor that 12km east to the Mu-River mouth, are used as representative waves.[1)]

According to wave heights and periods observed at water depth 50.7m off the East Tomakomai Harbor, although large waves which heights in the range of 1.5 ~ 3.88m and periods in the range of 4.9 ~ 6.6s appear offshore at least once a month, on the average significant wave height 0.72m and significant wave period 5.47s are used in the present study.

According to wave direction data from the Tomihama Harbor, wave directions in spring are as the same characteristics as in autumn. Whereas, in summer and winter, although the predominant direction is SW as the same in spring and autumn, WSW in summer and SSW in winter are also important.

## 3. The method of one-line model

One-line model is composed of wave propagation model and sand transportation model.

Wave forces at breaking point are considered as the main power to transport sand along shoreline. Wave forces are related to wave height, wave direction and wave group velocity at breaking point. Thus, in wave propagation model the key is how to correctly evaluate the wave factors at breaking point from wave conditions offshore. In natural coast, wave shoaling and refraction are the major causes make wave height higher as waves reach breaking point. While there are some artificial constructures in the shallow water, wave diffraction has to be taken into account behind the constructures. Based on the computed results of regular wave refraction, shoaling and diffraction, the significant wave factors of irregular waves should be calculated.

### 3.1. Wave Propagation Model

Equations for regular wave refraction computation are used as follows,

$$\frac{\partial\theta}{\partial s}=\frac{1}{k}\frac{\partial k}{\partial n}=-\frac{1}{C}\frac{\partial C}{\partial n} \tag{1}$$
$$=\frac{1}{C}(\sin\theta\frac{\partial C}{\partial x}-\cos\theta\frac{\partial C}{\partial y})$$

$$\frac{\partial^2\beta}{\partial s^2}+p\frac{\partial\beta}{\partial s}+q\beta=0 \tag{2}$$

In which,

$$p(s)=-\frac{\cos\theta}{C}\frac{\partial C}{\partial x}-\frac{\sin\theta}{C}\frac{\partial C}{\partial x} \tag{3}$$

$$q(s)=\frac{\sin^2\theta}{C}\frac{\partial^2 C}{\partial x^2}- \tag{4}$$
$$2\frac{\sin\theta\cos\theta}{C}\frac{\partial^2 C}{\partial x\partial y}+\frac{\cos^2\theta}{C}\frac{\partial^2 C}{\partial y^2}$$

and $\theta$ is wave direction; $k$ is wave number; $n$ and $s$ are unit vectors in wave direction and normal to wave direction, respectively; $C$ is wave celerity; $\beta = b / bo = 1 / K_R^2$, b and bo are widths of wave ray effect near the shore and offshore,respectively; $K_R$ is wave refraction coefficient.

Wave diffraction coefficient of regular waves behind semi-infinite long breakwater is calculated as[7)]

$$K_D=I(-\sqrt{\frac{4kr}{\pi}}\sin\frac{\alpha-\theta}{2})e^{-ikr\cos(\alpha-\theta)}$$
$$+I(-\sqrt{\frac{4kr}{\pi}}\sin\frac{\alpha+\theta}{2})e^{-ikr\cos(\alpha+\theta)} \tag{5}$$

In which,

$$I(\lambda)=\frac{1+i}{2}\int_{-\infty}^{\lambda}e^{-i\frac{\pi\lambda^2}{2}}d\lambda \tag{6}$$

$\alpha$ and $\theta$ are angles as shown in Fig. 2; $\gamma$ is the distance from the computation point to the head of semi-infinite long breakwater in polar coordinates.

Refraction of irregular waves is computed using the traditional method.[8-10)]

$$(K_R)_{eff}= \tag{7}$$
$$\{\frac{1}{m_{so}}\int_0^{\infty}\int_{\theta_{min}}^{\theta_{max}}S(f,\theta)K^2s(f)K^2R(f,\theta)d\theta df\}^{\frac{1}{2}}$$

In which,

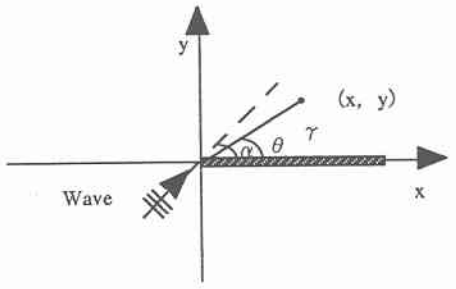


**Fig. 2 Wave Diffraction behind a Semi-infinite long Breakwater**

$$m_{so} = \int_0^{\infty}\int_{\theta_{min}}^{\theta_{max}} S(f,\theta)Ks^2(f)\,d\theta\,df \tag{8}$$

$f$, $\theta$ are wave frequency and direction, respectively; $Ks(f)$ is the wave shoaling coefficient of regular wave; $S(f,\theta)$ is a density function of direction spectrum and is given as ,

$$S(f,\theta) = S(f)G(\theta|f) \tag{9}$$

In which, $S(f)$is wave frequency spectrum,[11]

$$S(f) = \beta_J H_{1/3}^{\ 2} T_P^{-4} f^{-5} \times \exp\{-1.25(T_P f)^{-4}\} \times \gamma^{\exp\{-(T_P f-1)^{-2}/2\sigma^2\}} \tag{10}$$

and $G(\theta|f)$is a direction distribution function and regularized as,[12]

$$\int_{-\pi/2}^{\pi/2} G(\theta|f) = 1 \tag{11}$$

$H_{1/3}$ and $T_{1/3}$ are significant wave height and period, respectively.

$$\beta_J \approx 0.0624\{1.094 - 0.01915\ln\gamma\} / \{0.230 + 0.336\gamma - 0.185(1.9+\gamma)^{-1}\} \tag{12}$$

$$T_P = T_{1/3}/\{1.0 - 0.132(\gamma+0.2)^{-0.559}\} \tag{13}$$

$$\sigma = 0.07(f \le f_m),\ 0.09(f > f_m) \tag{14}$$

$$\gamma \cong 1 \sim 7 \tag{15}$$

$$G(\theta|f) = G_0 \cos^{2s}(\frac{\theta}{2}) \tag{16}$$

$S$ is a parameter means the concentration of directions.

$$G_0 = \frac{1}{\pi} 2^{2s-1} \frac{\Gamma^2(s+1)}{\Gamma(2s+1)} \tag{17}$$

$$\Gamma(S+1) = \int_0^{\infty} y^S e^{-y}\,dy \tag{18}$$

$$\Gamma(2S+1) = \int_0^{\infty} y^{2S} e^{-y}\,dy \tag{19}$$

$$S = 11.5\tilde{f}^{-2.5} \qquad \tilde{f} > \tilde{f}_m \tag{21}$$

$$S = 11.5\tilde{f}_m^{-7.5}\tilde{f}^{S} \qquad \tilde{f} \le \tilde{f}_m \tag{22}$$

Based on Mitsuyasu[12], if $S_{max}$ is given according to various waves, the following formula can be used to compute nondimensional frequency $\tilde{f}$ and peak nondimensional frequency $\tilde{f}_m$.

$$\tilde{f} = 2.656 S_{max}^{-0.4} f_m^{-1} f \tag{23}$$

$$\tilde{f}_m = 2.656 S_{max}^{-0.4} \tag{24}$$

In which $f_m$ is peak wave frequency.

When computing diffraction coefficient of irregular waves, just set shoaling coefficient $Ks(f)$=1.0 in equation (7 ), the others are the same as refraction coefficient computation.

Wave shoaling coefficient is calculated as

$$(K_S)_{eff} = 4.0\sqrt{m_{so}} \tag{25}$$

Wave heights at breaking point and before breaking in computation model are set as

$$H_b = K_D(\theta_1,h_b)K_R(\theta_1,h_b)K_S(h_b)H_{b-1} \tag{26}$$

$$H_{b-1} = K_D(\theta_1,h_{b-1})K_R(\theta_1,h_{b-1})K_S(h_{b-1})H_{b-2} \tag{27}$$

In which $H_b$ is wave height at breaking point, and $H_{b-1}$ is wave height at a grid point offshore and next to the breaking point. And moreover, $H_{b-2}$ is further off the breaking point. The same concept is used in the other points.

Wave breaking point is determined by applying Goda's Formulae as

$$\frac{H_b}{Lo} = 0.17[1 - \exp\{-1.5\frac{\pi h_b}{Lo}(1+15\tan(4/3\beta)\}] \tag{28}$$

In which, $Lo$is wave length offshore, $h_b$ is water depth at breaking point; $\beta$ is the slope of sea bed near shore on the average.

As shown in Fig. 3, Wave direction at break-

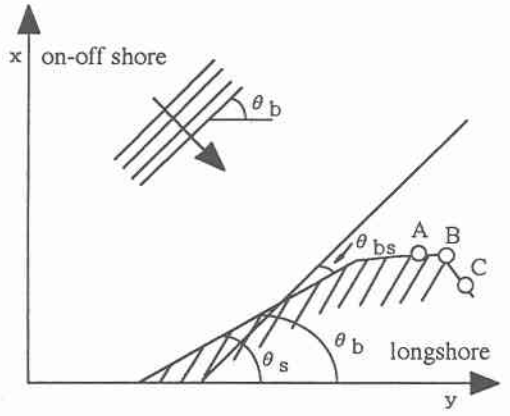


**Fig. 3 The Definition of Wave Direction at Breaking Point**

ing point is calculated in the following way,

$$\theta_{bs} = \theta_b - \theta_s = \theta_b - \tan^{-1}(\partial x / \partial y) \quad (29)$$

In which $\theta_{bs}$ is the angle between wave ray and shoreline; $\theta_b$ and $\theta_s$ are angles between wave ray and y-axis, and shoreline and y-axis, respectively. And as shown in Fig. 3, $\theta_s$ at point B should be given as the same as at point A, it should not be related to point C. Similarly, if $\theta_b$ changes or the shoreline direction sharply changes into another direction, $\theta_s$ and $\theta_{bs}$ can be determined as the method above.

### 3.2. Sand transportation model

As shown in Fig. 4, Sand transportation model is based on the sand conservation equation as follows.

$$\frac{\partial x}{\partial t} + \frac{1}{D}\left(\frac{\partial Q}{\partial y} - q\right) = 0 \quad (30)$$

In which, $Q$ is the volume of littoral drift that containing pores; $q : q = q_s + q_o$, $q_s$ is the quantity of sand transportation per unit meter along shoreline that from river or inland, and $q_o$ is sand from the sea; And $x$ is the shoreline position from specific line y-axis, where y is the coordinate in the direction of shoreline; $D$ is the critical water-depth of sand motion.[13]

$$D = 2.9Ho / \sqrt{\frac{\rho_s}{\rho} - 1 - 110Ho^2 / [(\frac{\rho_s}{\rho} - 1) g T_{1/3}^2]} \quad (31)$$

In which, $\rho_s$, $\rho$ are densities of sand and sea water, respectively; $Ho$ is significant wave height offshore; g is gravity acceleration.

Littoral drift between two adjacent points along shoreline are evaluated using the following Formulae.

$$Q = (H_b^2 C_g)_b (K_1 \sin 2\theta_{bs} - K_2 \cos\theta_{bs} \frac{\partial H_b}{\partial y}) \quad (32)$$

In which,

$$K_1 = K_{11} / [16(\frac{\rho_s}{\rho} - 1)(1 - \lambda) 1.416^{5/2}] \quad (33)$$

$$K_2 = K_{22} / [8(\frac{\rho_s}{\rho} - 1)(1 - \lambda) \tan\beta 1.416^{5/2}] \quad (34)$$

and $C_g$ is wave group velocity; $\lambda$ is sand porosity, and commonly given as 0.6. The value $1.416^{5/2}$ is a coefficient produced when computing significant wave height from the square of the average wave height. If $K_{22}$ is zero, and $K_{11}$ is 0.77, which means no constructures affect the shoreline, Formulae (32) is as the same as CERC's Formulae.

Correspondingly, one-line model is constructed as shown in Fig. 5.

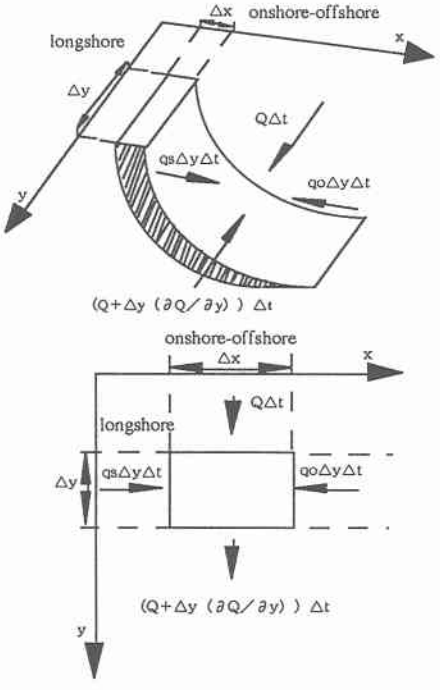


**Fig. 4 Principle Sketch of Shoreline Changes**

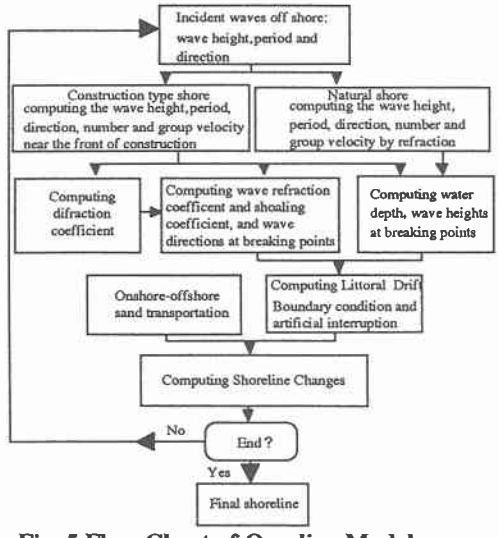


**Fig. 5 Flow Chart of One-line Model**

## 4. Computation Conditions

Computation area is limited in the range of 2.0km from offshore to the river mouth, and 2.8km from the left hand side to the right hand side. Two sets of grid points are tested when computing regular waves using significant waves. There are 2000 × 2800 points in one set, and space discretisation is set equal to 1m in longshore direction and on-off shore direction. In the other one 400 × 560 points are set up, and the interval length between two neighboring points is 5m. Although wave heights, wave group velocities and wave directions are different at breaking points of two sets, the differnces between their comprehensive effects to litroral drift are not obvious. Hence, in order to shorten computation time, the second one is applied in this research in practice.

When computing irregular waves, wave frequency is divided into 36 using energy average-dividing method, and wave direction is divided into 36 in the range from - $\pi$ /2 to $\pi$ /2.

In sand transportation model, computation area is separated into two areas. The river mouth is set as the boundary of two areas based on that river discharge cuts off the continuity of longshore current. Littoral drift of points on and near the breakwater of the Shiomi Fishery Port is set to be zero, and on the most right hand side of the river mouth, littoral drift is presupposed as the same as points that next to the boundary points. Littoral drift on the boundary of the river mouth is set by using linear outer-polation method. 25m is adopted as the interval length of neighboring points along shoreline, as the profile of shoreline changes sharply in some place, wave direction would be mis-evaluated at breaking points shown in Fig. 2 if computation points are depopulated more.

Sediment of the river discharge is neglected in this research because of 500m$^3$/year in traction state, and suspended sand should be transported further into the sea because of the influences of wedge of salt water. As almost no constructures affect this area, $K_{11}$=0.77 and $K_{22}$=0 are set in Formulae (32).

## 5. Results and Discussion

According to the observed data, sand deposited on the left hand side of the river mouth, the maxi-

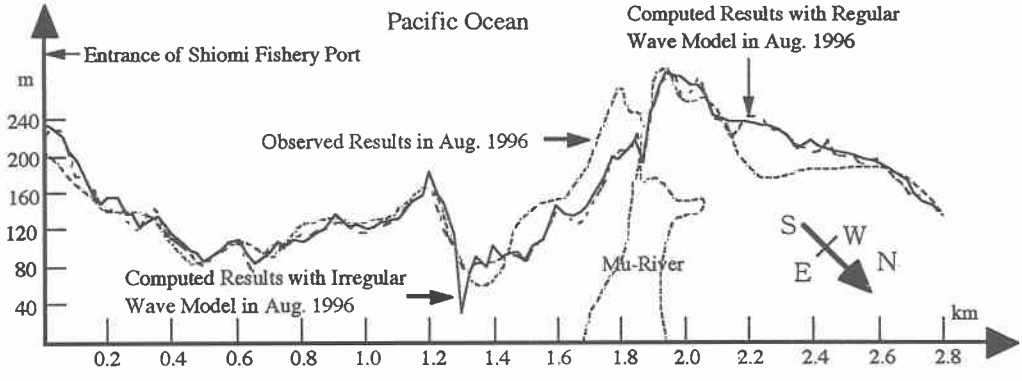


**Fig. 6 Comparisons of Computed Results and Observed Results**

mum value of shoreline propagation can reach 60m; while the shoreline on the right hand side of the river mouth had been eroded, the maximum value of shoreline recession is 60m, too . Comparing the computed data to the observed data, as shown in Fig. 6, differences between observed results and computed results of shoreline changes appear around breakwater of the Shiomi Fishery Port and around the river mouth, and good agreement at other areas, which means that the computed data can reproduce the trend of the shoreline changes using the significant waves. And there are no so many differences between results of regular wave model and irregular wave model.

The disagreement can be considered as ignored the sand transportation from inland around the river mouth and influences of higher waves during Feb. to Aug. 1996. And in fact, the interaction between river sediment discharge and littoral drift is still not well understood nowadays.

## 6. Conclusions

Based on the research above, conclusions can be made as,

1) The utility of one-line model is verified by applying regular and irregular wave deformation model from the study on shoreline changes of the Mu-River mouth during from Feb. to Aug. 1996.

2) Unusually higher wave conditions and interaction between littoral current and river sediment discharge should be taken into account in order to predict shoreline changes around a river mouth more correctly.

## Acknowledgments

Many thanks should be given to Mr. President Akira Kawamori, and Mr. Ken-ichi UJII of Alfa Hydraulic Engineering Consultants Company, for giving the senior author very useful advice.

## References

1) Report on investigation of the Tomakomai Harbor, Hokkaido developing Bureau, Muroran developing and construction department, Office of Tomakomai Harbor construction, 1997.( in Japanese)

2) Report on investigation of the Mu-River way characteristics, Muroran developing and construction department, 74,1991. ( in Japanese)

3)Tanaka Norio and K. Nadaoka: Predict model developing on shoreline and its application in real field. Materials of the Port and Harbor Research Institute,1982.(in Japanese)

4) Kraus N.C.:Applications of shoreline prediction model, Proc. Coastal Structures '83, ASCE, 632-645,1982.

5) Kraus N.C., and S. Harikai: Numerical model of the shoreline change at Oarai Beach, Coastal Engineering, 7,1,1-28,1983.

6) Kraus N.C., M. Isobe, H. Igarashi, T. Sasaki and K. Horikawa: Field experiments on longshore sand transport in the near shore zone, Proc. 18th CEC,969,988,1982

7) Predict Model on Coast variation, Associate of Electricity Business, Coast and Hydraulic research Committee, Japan, 1984.( in Japanese)

8) Goda Y., T. Takayama and Y. Suzuki: Diffraction diagrams for directional waves, Proc. 16th Coa. Eng. Conf. ASCE,628-650, 1978.

9) Nagai Kohei : Computation of refraction and diffraction of irregular sea waves, Report of the Port and Harbor Research Institute, Vol. 11, No. 2,1972. (in Japanese)

10) Goda Y. and Y. Suzuki: Computation of refraction and diffraction of sea waves, with Mitsuyasu's directional spectrum, 1975.(in Japanese)

11) Goda Y. : Specific spectrum and statistic characteristic of waves affected by numerical simulation, Proc. of the 34th Japanese Conference on Coastal Eng., 131-135,1987.( in Japanese)

12) Mitsuyasu T., etc.: A study on wave directional spectrum, Proc. of the 20th Japanese Conference on Coastal Eng., 435-439,1973.( in Japanese)

13) Hallermeier A.J.: Sand transport limits in coastal structure design, Proc. Coastal Structures ' 83, ASCE,703-716,1983.